*Desalination and Water Treatment*
www.deswater.com

doi: 10.5004/dwt.2018.22320

118 (2018) 135–142
June

# Effect of pH on 17 beta-estradiol adsorption by anaerobic granule sludge combined with iron

Bai-Hang Zhao[a,*], Zhan-Zhao Wang[a], Jing Zhang[a], Jun Li[a], Jie-Yi Zhai[a], Wei Bian[a], Wei-Hua Li[b], Xian-Huai Huang[b]

[a]*Department of Municipal Engineering, Beijing University of Technology, Beijing 100124, China, emails: bhzh@bjut.edu.cn (B.H. Zhao), wangzhanzhao@emails.bjut.edu.cn (Z.Z. Wang), b201604017@emails.bjut.edu.cn (J. Zhang), jglijun@bjut.edu.cn (J. Li), jieyizhai@126.com (J.Y. Zhai), yangzhoubw@126.com (W. Bian)*

[b]*School of Environment and Energy Engineering, Anhui Jianzhu University, Hefei 230601, China, emails: weihuali0311@126.com (W.H. Li), xianhuaihuang@126.com (X.H. Huang)*

Received 8 October 2017; Accepted 5 April 2018

---

**ABSTRACT**

Estrogens have great harmfulness to living organisms. Adsorption is a key step to estrogen removal in biological process. As a typical estrogen with high estrogen activity, 17 beta-estradiol (E2) adsorption behavior by anaerobic granular sludge (AnGS) combined with zero-valent iron (ZVI) was researched here. The effect of pH on E2 adsorption by ZVI/AnGS was investigated and analyzed through adsorption equilibrium, adsorption kinetics, adsorption thermodynamics, and zeta potential. ZVI/AnGS had high E2 adsorption capacity. The optimized condition was pH 6 with 92.78% E2 adsorption efficiency, 4.95 μg·gVSS$^{-1}$ equilibrium adsorption capacity, and 0.07 g·μg$^{-1}$·min$^{-1}$ adsorption rate. E2 was adsorbed as cationic forms or neutral inner-sphere surface complexes at a pH range of 2–10. The adsorption rate was controlled by film diffusion or intraparticle diffusion. Freundlich and Langmuir isotherms were both suitable for describing E2 adsorption process, which was exothermic and spontaneous.

*Keywords:* Estrogen; Adsorption; pH; Anaerobic granular sludge; Zero-valent iron

---

## 1. Introduction

Estrogens are important environmental contaminants that disrupt endocrine systems and feminize male fish. A lot of attentions have been focused on estrogen's fate and removal in biological systems, especially in activated sludge systems [1–3], owing to estrogen flow into wastewater treatment plant with domestic wastewater. Estrogen transformation in strictly anaerobic environment has also been reported by many researches. The reports about estrogen's anaerobic transformation are related to estrogen transformation in sludge anaerobic digester [4,5], in livestock wastewater or dairy lagoon water treatment process [6,7], in anaerobic membrane bioreactors [8], and so on. It indicates estrogens can be removed during anaerobic digestion process [4,9].

As we all know, adsorption is the first step for organic pollutant's biological removal. Biodegradation step often happens after adsorption step of organic pollutants by biological aggregates. Adsorption plays an important role about estrogen removal in activated sludge treatment system [10,11]. The adsorption process is also crucial to estrogen removal in anaerobic systems [12]. More attentions have been focused on estrogen's adsorption by floc sludge [13,14], with relatively little attention on granular sludge, especially anaerobic granular sludge (AnGS). In fact, AnGS has relatively high estrogen adsorption efficiency with a 60.54% of 17 beta-estradiol (E2) removal [15].

Estrogen removal process is affected by pH, temperature, ion strength, hydraulic retention time, and other operating

---

* Corresponding author.

1944-3994/1944-3986 © 2018 Desalination Publications. All rights reserved.

factors [16,17]. Among them, pH is considered to be a significant influence factor [16]. pH changes the electrostatic repulsion on the surface of adsorbent and causes the changes of adsorption efficiency and adsorption capacity [18]. Urase et al. [19] observed an increase of E2 adsorption by activated sludge accompanied with a decrease of pH. Zhang et al. [20] found Estriol (EE2) adsorption capacity was almost unchanged at pH 3–10 and sharply decreases with pH > 10 with sludge derived from different treatment units as adsorbent. Chen et al. [14] pointed out the adsorption capacity of estrone and E2 to activated sludge was the highest at neutral pH. Above researches show that pH has different impact trends on estrogen adsorption removal at different batch experiments. Little information about pH effect on estrogen removal by AnGS can be found.

Zero-valent iron (ZVI) has been widely and successfully applied into wastewater anaerobic biological treatment process for removing persistent organic pollutant [21]. Zhao et al. [22] reported an increase of 48% for E2 adsorption by AnGS was obtained after ZVI addition. It indicates ZVI has the ability to enhance E2 adsorption by AnGS. E2 is a typical natural estrogen with high estrogen activity. Hence, we investigated the effect of pH on estrogen adsorption by AnGS combined with ZVI (ZVI/AnGS) using E2 as representative. An optimized pH was obtained according to a high adsorption efficiency and adsorption capacity of ZVI/AnGS to E2. The effect of pH on E2 adsorption by ZVI/AnGS was analyzed through adsorption equilibrium, adsorption kinetics, and adsorption thermodynamics, also with zeta potential.

## 2. Materials and methods

### 2.1. Chemicals

17 beta-estradiol-2,4,16,16-d4 (E2-d4) was used as an internal standard substance in the analysis process of E2 by gas chromatography-mass spectrometry (GC-MS). The E2, E2-d4, and BSTFA (1% TMCS) were of an analytical reagent grade purchased from Sigma, Germany. Other organic solvents including methanol and ethyl acetate were of chromatographic reagent grade from Sinopharm, China. High-purity water was produced using a Milli-Q Plus system (Millipore, USA)

### 2.2. Adsorption experiment

AnGS was taken from a UASB reactor treating beer wastewater in Yanjing Brewery, which is located at Shunyi District of Beijing. The sludge was washed with pure water and centrifuged at 3,600 rpm for 15 min to remove water-soluble constituents. Organic pollutant's adsorption process by biological treatment has often been investigated by inactivated organism to eliminate the effect of biodegradation [11,13]. Before our adsorption experiments, the AnGS was frozen at –40°C for 10 h and inactivated by autoclaving at 121°C for 30 min to eliminate E2 removal through biodegradation.

The effect of pH on estrogen adsorption by ZVI/AnGS was investigated by setting a series of batch tests with a pH range of 2–10. The batch tests were carried out in a 250 mL serum bottles with a 200 mL working volume. Except for pH, all environment conditions and operation process in ZVI and AnGS system were kept the same as that in ZVI/AnGS systems in order to compare the effect of ZVI, AnGS, and ZVI/AnGS on E2 adsorption. E2 initial concentration, AnGS concentration, ZVI concentration, and temperature were 8 µg·L$^{-1}$, 1.5 gVSS·L$^{-1}$, 2 g·L$^{-1}$, and 25°C, respectively, in the serum bottles. E2, inactivated AnGS, and ZVI were added into the serum bottles in turn. Then, initial pH was adjusted by adding 2 mol·L$^{-1}$ NaOH or 2 mol·L$^{-1}$ HCl. After that, the bottles were blown for 5 min with high-purity nitrogen (99.999%) to remove dissolved oxygen and maintain strictly anaerobic environment. Then, the serum bottles were quickly sealed with rubber plugs and shaken in a constant temperature oscillator at 120 rpm (Jintan Medical Instrument Factory, BS-1E, China) for 2 h to ensure adsorption equilibrium was reached.

E2 adsorption by ZVI/AnGS was analyzed in terms of E2 adsorption efficiency ($R_{\text{removal}}$) and the adsorption capacity of ZVI/AnGS to E2 ($q_e$), which were calculated as follows (Eqs. (1) and (2)):

$$R_{\text{removal}} = \frac{C_0 - C_i}{C_0} \times 100 \tag{1}$$

$$q_t = \frac{(C_0 - C_i)}{W} \cdot V \tag{2}$$

where $C_0$ (µg·L$^{-1}$) and $C_i$ (µg·L$^{-1}$) are initial E2 concentration and E2 concentration at time $t$, respectively; $q_i$ (µg·gVSS$^{-1}$) is the amount of adsorbed E2 per gram of AnGS at time $t$; $W$ (gVSS) represents AnGS dry weight; and $V$ (L) represents the working volume.

### 2.3. Kinetic adsorption

Adsorption is a time-dependent process. The adsorption rate of a pollutant is an important parameter to evaluate the feasibility of the adsorbent for use in wastewater treatment. To evaluate the adsorption rate and adsorption dynamics mechanism of E2 adsorption by AnGS, two kinetic models were used to describe the adsorption data in our experiment.

The pseudo-first-order kinetic model is as follows:

$$\lg\left(q_e - q_t\right) = \lg q_t - \frac{k_1 . t}{2.303} \tag{3}$$

The pseudo-second-order kinetic model is as follows:

$$\frac{t}{q_t} = \frac{1}{k_2 q_e^2} + \frac{t}{q_e} \tag{4}$$

where $q_e$ (µg·gVSS$^{-1}$) is the adsorption capacity when adsorption equilibrium is reached; $k_1$ (min$^{-1}$) is the adsorption rate constant of the pseudo-first-order model; and $k_2$ (g·µg$^{-1}$·min$^{-1}$) is the adsorption rate constant of the pseudo-second-order model.

### 2.4. Adsorption isotherm models

The adsorption phase equilibrium explains the maximum adsorption capacity of the adsorbent for the adsorbate molecule and the adsorption selectivity. The type of adsorption isotherm and their corresponding parameter provide important basis for designing and optimizing an adsorption system. The adsorption equilibrium data in our experiments were evaluated by Langmuir and Freundlich isotherms to describe the interaction of E2 and AnGS when equilibrium was reached between the liquid and solid phases.

The Langmuir isotherm equation is as follows:

$$q_e = \frac{q_{\max} \cdot b \cdot C_e}{1 + b \cdot C_e} \tag{5}$$

where $q_{\max}$ (μg·gVSS$^{-1}$) is the maximum adsorption capacity of AnGS; $b$ (L·μg$^{-1}$) is the adsorption equilibrium constant.

The Freundlich isotherm equation is as follows:

$$q_e = K_f C_e^{1/n} \tag{6}$$

where $K_f$ (L·gVSS$^{-1}$) is a constant related to the AnGS adsorption capacity; $n$ is an empirical parameter related to adsorption intensity, which changes with the adsorbent's heterogeneity.

### 2.5. Adsorption thermodynamic

To further study the effect of pH on E2 adsorption by AnGS, the thermodynamic behavior was investigated and analyzed by Gibbs equation. The Gibbs free energy exchange ($\Delta G^o$), adsorption entropy exchange ($\Delta S^o$), and adsorption enthalpy exchange ($\Delta H^o$) in the adsorption process were calculated using the following equations:

$$K_d = \frac{q_e}{C_e} \tag{7}$$

$$\ln K_d = \frac{\Delta S^o}{R} - \frac{\Delta H^o}{R \cdot T} \tag{8}$$

$$\Delta G^o = \Delta H^o - T \cdot \Delta S^o \tag{9}$$

where $K_d$ is the distribution coefficient of E2 in the solid and liquid phase at equilibrium; $R$ (kJ·mol$^{-1}$·K$^{-1}$) is the ideal gas constant (8.314 × 10$^{-3}$); $T$ (K) is absolute temperature; $\Delta G^o$ (kJ·mol$^{-1}$) is the Gibbs free energy; $\Delta S^o$ (kJ·mol$^{-1}$·K$^{-1}$) is the standard entropy change; and $\Delta H^o$ (kJ·mol$^{-1}$) is the standard enthalpy change.

### 2.6. Analysis

E2 was measured by GC-MC (Agilent 6890N-5973, USA). The reaction solution was filtered through a 0.45 μm glass fiber membrane (Jinteng, China). The pH of the filtered water sample was adjusted to 2.0–3.0 by 10% HCl. Solid phase extraction (SPE) was used to extract E2 in the filtered samples. The SPE column was activated in turn by 5 mL ethyl acetate, 5 mL methanol, and 10 mL ultra-pure water before use. The E2 in the filtered water sample was enriched in the activated SPE column with a flow rate of 5 mL·min$^{-1}$. The SPE column was eluted by 10 mL methanol, and 10 mL ethyl acetate was used to extract E2 enriched in the SPE column. The extraction solution was collected in a bottle with 2 mL volume and inundated slowly with nitrogen at 45°C. E2 in the bottle was treated with 100 μL BSTFA (1% TMCS) for 30 min and then with 50 μL pyridine at 70°C. The derived sample was measured by GC-MC (Agilent 6890N-5973, USA) after cooling to room temperature. The sample injection volume was 10 μL.

The gas chromatography was conducted using an Agilent DB-FFAP (122-3232) (0.25 mm × 30 mm, film thickness 0.25 μm) with helium as a carrier gas at a flow rate of 1.0 mL·min$^{-1}$. The inlet temperature was set to 250°C, and the initial temperature of ramping oven was set to 100°C for 1 min. The temperature of the ramping oven was raised to 200°C at a rate of 10°C·min$^{-1}$ and then to 300°C at a rate of 3°C·min$^{-1}$. The mass spectrometer conditions were ionization mode, EI, with electron energy at 70 eV, interface temperature of 280°C, ion source temperature of 230°C, quadrupole temperature of 150°C, and a solvent delay of 15 min.

The zeta potential of AnGS combined with ZVI before and after the adsorption was measured using Zeta-Potential Analyzer (90Plus, Brookhaven Instruments Corp., Holtsville, NY, USA). The value of zeta potential at the same conditions was measured three times, and average values were used here. The value of E2 concentration and zeta potential at the same conditions were measured three times, and average values were used here.

## 3. Results and discussion

### 3.1. The adsorption behavior of E2 by ZVI/AnGS

E2 adsorption behavior by ZVI, AnGS, and ZVI/AnGS was investigated, respectively. Fig. 1 shows the change of adsorption capacity with time in different systems (ZVI, AnGS, and ZVI/AnGS) at pH 6. When the adsorption equilibrium was reached, the adsorption capacities of ZVI, AnGS, and ZVI/AnGS to E2 were 1.23, 4.14, and 6.12 μg·gVSS$^{-1}$, respectively. E2 removal was poor in ZVI system, but high in ZVI/AnGS system. Not only the adsorption capacity of ZVI/AnGS system was 47.8% higher than that of AnGS system,

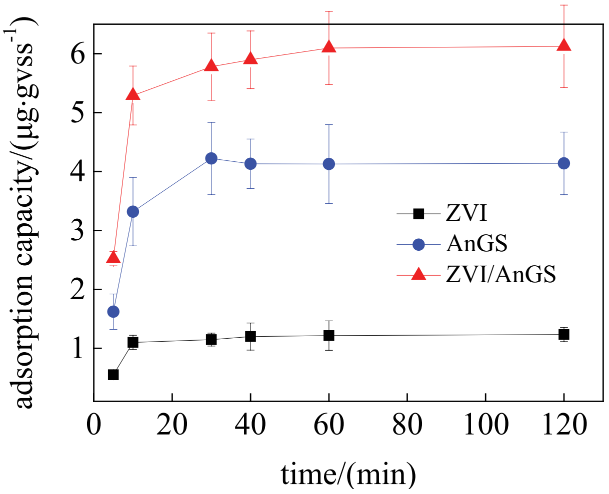

Fig. 1. The change of adsorption capacity in different systems with time.

but it was 14.0% higher than the adsorption capacity sum of ZVI system and AnGS system. This exposed that ZVI addition increases E2 adsorption by AnGS. There was a synergistic effect between ZVI and AnGS to E2 adsorption. The percentage of E2 adsorption by ZVI, AnGS, or the synergistic effect between ZVI and AnGS in ZVI/AnGS system was about 20.1%, 67.6%, or 12.3% calculated by the adsorption capacity of ZVI, AnGS, and ZVI/AnGS to E2.

### *3.2. Effect of pH on E2 adsorption by ZVI/AnGS*

The effect of pH on E2 adsorption by ZVI/AnGS was investigated with a pH range of 2–10. As shown in Fig. 2(a), the adsorption capacity was increasing with time at different pH. When pH increased from 2 to 6, a small fluctuating variation was observed for E2 adsorption efficiency and the equilibrium adsorption capacity (Fig. 2(b)). When pH increased from 6 to 10, E2 adsorption efficiency and the equilibrium adsorption capacity sharply decreased from 92.78% to 50.61% and from 4.95 to 2.70 μg·gVSS$^{-1}$, respectively. A high E2 adsorption efficiency (92.78%) and a high equilibrium adsorption capacity (4.95 μg·gVSS$^{-1}$) for ZVI/AnGS system were simultaneously obtained at pH 6.

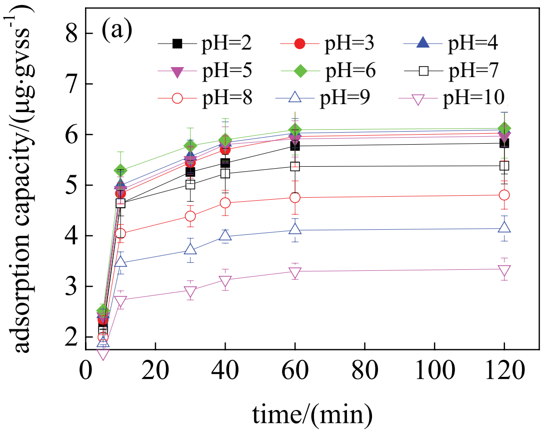

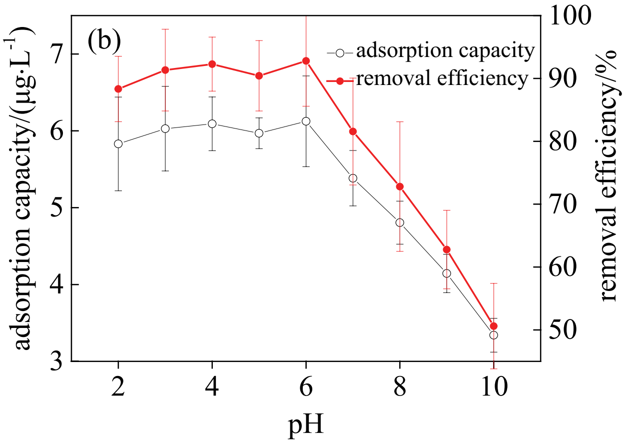

Fig. 2. Effect of pH on E2 adsorption by ZVI/AnGS: (a) the change of adsorption capacity with time and (b) adsorption capacity and adsorption efficiency at different pH.

Clara et al. [16] point out that negative surface charges of adsorbent are neutralized by hydrogen ions and cause the reduction of thermodynamic potential in adsorption process. Low pH brought more hydrogen ions in favor of E2 adsorption by AnGS. ZVI corrosion more likely occurs at lower pH, accompanied with production of lots of hydrogen molecules. The large amount of hydrogen molecules might affect the contact between E2 and AnGS [23]. The positive effect of low pH and the negative effect of hydrogen molecules on E2 adsorption by AnGS cancel each other in the adsorption process. Therefore, a little change existed for E2 adsorption efficiency and the equilibrium adsorption capacity when pH increased from 2 to 6. This suggested that ZVI addition eliminated the effect of pH on E2 adsorption by AnGS at low pH range. Besides hydrogen molecules, $Fe^{2+}$ and $Fe^{3+}$ are produced in ZVI corrosion process. These ions tend to react with hydroxyl and formed colloids at high pH, such as $Fe(OH)_2$, $Fe(OH)_3$, $Fe(H_2O)_x^{2+}$, and $Fe(H_2O)_x^{3+}$, which might block the aperture of AnGS and occupy effective adsorption sites on AnGS's surface [24]. The above action of colloids led to the decrease of E2 adsorption efficiency and the equilibrium adsorption capacity at high pH for E2 adsorption by ZVI/AnGS.

### *3.3. Adsorption kinetic studies at different initial pH*

The pseudo-first-order model and pseudo-second-order model were used to describe E2 adsorption process at different pH to evaluate the adsorption rate and adsorption dynamics mechanism of ZVI/AnGS to E2. The values of $q_e$, $k_1$, and $k_2$ in Eqs. (3) and (4) were calculated according to the slope and intercepts of straight line plots of $\lg(q_e - q_t)$ or $t/q_t$ versus $t$ (Fig. 3). All parameter values, including the theoretical adsorption capacity ($q_{e,\mathrm{cal}}$) and experimental adsorption capacity ($q_{e,\mathrm{exp}}$), are summarized and listed in Table 1. The values of $q_{e,\mathrm{cal}}$ calculated by Eq. (2) were far from the $q_{e,\mathrm{exp}}$ values. The values of $q_{e,\mathrm{cal}}$ calculated by Eq. (3) were closer to the $q_{e,\mathrm{exp}}$ values. The $R^2$ values for pseudo-first-order model ranged from 0.937 to 0.958. The $R^2$ values for the pseudo-second-order model were between 0.993 and 0.999. The $R^2$ values of the pseudo-second-order model were higher than those of the pseudo-first-order model. The higher $R^2$ values and similar $q_{e,\mathrm{cal}}$ and $q_{e,\mathrm{exp}}$ values prove that the pseudo-second-order model was better suited to describe E2 adsorption process by ZVI/AnGS compared with the pseudo-first-order model.

The pseudo-second-order model basically includes all steps of adsorption such as external film diffusion, intraparticle diffusion, and adsorption reaction. The step of adsorption reaction is always considered to be rapid and to be negligible. Hence, the overall adsorption rate of E2 by ZVI/AnGS was controlled by film diffusion or intraparticle diffusion.

When pH increased from 2 to 6, the values of $q_{e,\mathrm{cal}}$ fluctuated between 6.07 and 6.31 μg·g$^{-1}$. A little change for $q_{e,\mathrm{cal}}$ was been observed with a pH range of 2–6. The $q_{e,\mathrm{cal}}$ declined from 6.31 to 3.46 μg·g$^{-1}$ with pH increasing from 6 to 10. The values of $k_2$ increased from 0.04 to 0.07 g·μg$^{-1}$·min$^{-1}$ with the raise of pH from 2 to 6, and then stay at 0.07 g·μg$^{-1}$·min$^{-1}$ until pH rises to 10. High adsorption rate was exited at a pH range of 7–9, but the adsorption capacity in the pH range was low than that at pH 6. It was simultaneously obtained a high adsorption rate and a high adsorption capacity of ZVI/AnGS to E2 at pH 6. The optimized condition of pH 6 according to kinetic analysis was consistent with that on the basis of the experiment data of effect of pH on E2 adsorption efficiency and the equilibrium adsorption capacity.

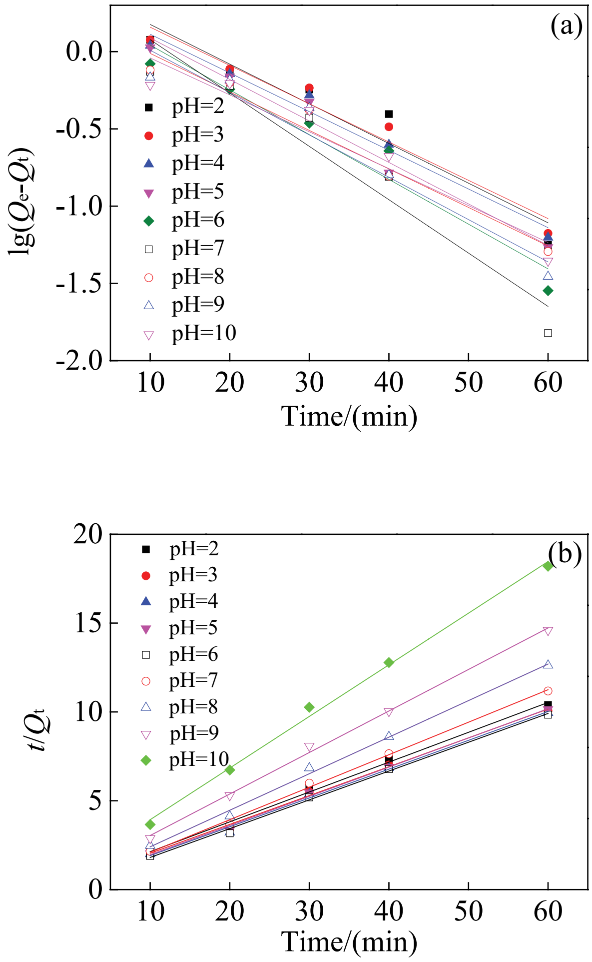

Fig. 3. Adsorption kinetic at different initial pH: (a) pseudo-first-order model and (b) pseudo-second-order model.

### 3.4. Adsorption isotherms at different initial pH

Freundlich isotherm and Langmuir isotherm (Eqs. (5) and (6)) were used to describe the adsorption experimental data at different pH. The coefficients of various isotherms are listed in Table 2. The $R^2$ values of Freundlich isotherms ranged from 0.970 to 0.998. The $R^2$ values of Langmuir isotherms were between 0.941 and 0.996. High values of $R^2$ were exited for both Freundlich isotherms and Langmuir isotherms. It means Freundlich and Langmuir isotherms were both suitable for describing the adsorption process of ZVI/AnGS to E2. But Freundlich isotherm was better than Langmuir isotherm to describe the adsorption process.

$K_f$ relates to the adsorption capacity of ZVI/AnGS to E2. A high $K_f$ value means a strength adsorption capacity. The values of $K_f$ were in a range of 1.046–5.679 at different pH (Table 2), which was comparable with the $K_f$ values of 2.62–3.10 or 3.13–3.44 about E2 adsorption using activated sludge or aerobic granular sludge, respectively [12]. This confirms ZVI/AnGS has a high adsorption capacity for E2. The values of $K_f$ gradually increased from 4.929 to 5.679 with a pH rise from 2 to 6 and then rapidly dropped to 1.046 with a pH decline from 6 to 10. A higher value of $K_f$ was obtained at pH 6, which was consistent with the optimal pH 6 for high E2 adsorption efficiency and high equilibrium adsorption capacity.

The constant $n$ is an empirical parameter associated with the degree of heterogeneity. A higher value of $n$ means a stronger adsorption bond exited between adsorbate and adsorbent [25]. A favorable adsorption occurs between adsorbate and adsorbent when $0.1 < n^{-1} < 1.0$ [26]. The values of $n^{-1}$ were in a range of 0.507–0.740, which reflected high adsorption intensity and binding force between AnGS and E2. Taken together, the values of $K_f$ and $n^{-1}$ in the adsorption process of E2 onto ZVI/AnGS at different pH demonstrate that E2 can be effectively adsorbed by ZVI/AnGS.

### 3.5. Adsorption thermodynamics at different initial pH

Table 3 shows thermodynamic parameters for the adsorption process of E2 onto ZVI/AnGS at different pH. The values of $\Delta G^o$, $\Delta S^o$, and $\Delta H^o$ in ZVI/AnGS system were all negative. The negative values of $\Delta H^o$ and $\Delta G^o$ demonstrated that the adsorption process of E2 onto ZVI/AnGS was exothermic and spontaneous. The negative values of $\Delta S^o$ suggested a more

Table 1
Kinetic constant for pseudo-first-order and pseudo-second-order model

| pH | Pseudo-first-order model | | | Pseudo-second-order model | | | $q_{e,\exp}$ (μg·g$^{-1}$) |
|---|---|---|---|---|---|---|---|
| | $q_{e,\text{cal}}$ (μg·g$^{-1}$) | $k_1$ (min$^{-1}$) | $R^2$ | $q_{e,\text{cal}}$ (μg·g$^{-1}$) | $k_2$ (g·(μg·min)$^{-1}$) | $R^2$ | |
| 2 | 3.85 | 0.07 | 0.943 | 6.07 | 0.04 | 0.998 | 5.83 |
| 3 | 3.94 | 0.07 | 0.956 | 6.27 | 0.04 | 0.999 | 6.03 |
| 4 | 3.48 | 0.07 | 0.958 | 6.31 | 0.05 | 0.999 | 6.09 |
| 5 | 3.39 | 0.07 | 0.958 | 6.10 | 0.05 | 0.999 | 5.97 |
| 6 | 3.40 | 0.08 | 0.939 | 6.19 | 0.07 | 0.993 | 6.12 |
| 7 | 3.56 | 0.09 | 0.943 | 5.56 | 0.07 | 0.996 | 5.38 |
| 8 | 2.52 | 0.07 | 0.942 | 4.95 | 0.07 | 0.998 | 4.81 |
| 9 | 2.35 | 0.07 | 0.945 | 4.30 | 0.07 | 0.997 | 4.14 |
| 10 | 1.78 | 0.06 | 0.937 | 3.46 | 0.05 | 0.996 | 3.34 |

Table 2
Adsorption parameters and correlation coefficients for different isotherm models at different pH

| pH | Freundlich | | | Langmuir | | |
|---|---|---|---|---|---|---|
| | $K_f$(μg·g$^{-1}$) | $n^{-1}$ | $R^2$ | $Q_{\max}$ (μg·g$^{-1}$) | $b$ (L·μg$^{-1}$) | $R^2$ |
| 2 | 4.929 | 0.507 | 0.998 | 7.886 | 2.042 | 0.950 |
| 3 | 5.558 | 0.535 | 0.993 | 8.354 | 2.172 | 0.943 |
| 4 | 5.561 | 0.541 | 0.992 | 8.511 | 2.072 | 0.946 |
| 5 | 5.606 | 0.620 | 0.970 | 9.452 | 1.198 | 0.946 |
| 6 | 5.679 | 0.568 | 0.989 | 8.865 | 1.880 | 0.941 |
| 7 | 3.432 | 0.589 | 0.993 | 8.264 | 0.844 | 0.972 |
| 8 | 2.321 | 0.740 | 0.995 | 11.148 | 0.279 | 0.996 |
| 9 | 1.585 | 0.698 | 0.987 | 8.389 | 0.242 | 0.988 |
| 10 | 1.046 | 0.712 | 0.995 | 7.246 | 0.165 | 0.993 |

Table 3
Thermodynamic parameters of E2 adsorption by ZVI/AnGS at different pH

| pH | $\Delta G^o$ (kJ·mol$^{-1}$) | | | | | | | $\Delta H^o$ (kJ·mol$^{-1}$) | $\Delta S^o$ (J·mol$^{-1}$·K$^{-1}$) |
|---|---|---|---|---|---|---|---|---|---|
| | 5°C | 10°C | 20°C | 25°C | 30°C | 35°C | 40°C | | |
| 2 | −19.40 | −19.34 | −19.28 | −19.23 | −19.17 | −19.11 | −19.06 | −22.57 | −11.39 |
| 3 | −22.23 | −22.17 | −22.10 | −22.04 | −21.97 | −21.91 | −21.84 | −25.86 | −13.02 |
| 4 | −23.53 | −23.46 | −23.39 | −23.33 | −23.26 | −23.19 | −23.12 | −27.37 | −13.78 |
| 5 | −21.44 | −21.38 | −21.31 | −21.25 | −21.19 | −21.13 | −21.06 | −24.94 | −12.57 |
| 6 | −22.57 | −22.50 | −22.43 | −22.37 | −22.30 | −22.24 | −22.17 | −26.24 | −13.19 |
| 7 | −17.18 | −17.12 | −17.07 | −17.02 | −16.97 | −16.92 | −16.87 | −20.03 | −10.25 |
| 8 | −13.75 | −13.71 | −13.67 | −13.62 | −13.58 | −13.54 | −13.50 | −16.06 | −8.30 |
| 9 | −21.82 | −21.87 | −21.92 | −21.97 | −22.02 | −22.08 | −22.13 | −19.01 | −10.10 |
| 10 | −14.40 | −14.35 | −14.31 | −14.26 | −14.21 | −14.17 | −14.12 | −16.97 | −9.23 |

ordered behavior or affinity of E2 on the sorbent at the solid–solution interface [27].

At 25°C, the $\Delta G^o$ values fluctuated within a range of −23.33 to −19.23 and −21.97 to 13.62 when pH increased from 2 to 6 and from 6 to 10, respectively (Table 3). Two distinct regions for $\Delta G^o$ values were observed in the pH range of 2–6 and 6–10 at 25°C. The $\Delta G^o$ value drastically jumped to −17.02 when pH increased from 6 to 7. Similar phenomenon about $\Delta G^o$ values appeared in other experiments with different temperature (Table 3), as well as about $\Delta H^o$ values and $\Delta S^o$ values. Low $\Delta G^o$ means high adsorption driving force [28]. The high-driving force in pH 6 resulted into a high adsorption capacity of ZVI/AnGS to E2.

### 3.6. Zeta potential before and after adsorption at different pH

The change of zeta potential can provide valuable information on the surface forms of adsorbates, since the formation of the surface complexes will change the surface charge. The zeta potential values before and after adsorption at different pH are shown in Fig. 4. The zeta potential values decreased from −0.0203 mV at pH 2 to −30.5333 mV at pH 6 and then rapidly increased to 0.0012 mV at pH 10 before adsorption. Similar trend was observed about the zeta potential change after adsorption. Two zero charge points (ZCPs) were found in our experiments, and they were near about pH 2 ($\mathrm{pH_{ZCP}}$ 2) at low pH range and pH 10 ($\mathrm{pH_{ZCP}}$ 10) at high pH (Fig. 4), respectively. Negative zeta potential value means negative electrostatic charges exist in the surface of adsorbents. At $\mathrm{pH_{ZCP}}\ 2 < \mathrm{pH} < \mathrm{pH_{ZCP}}\ 10$, zeta potential values were all negative. It indicates the surface of AnGS gets negatively charged, thereby supporting more E2 uptake due to electrostatic force of attraction [29]. Lower zeta potential means better adsorption removal caused by electrostatic force. The zeta potential value at pH 6 was lower than that at other pH. The lower zeta potential value at pH 6 results in the higher E2 adsorption by ZVI/AnGS.

The formation of charged inner-sphere surface complexes changes the zeta potential values and the $\mathrm{pH_{ZCP}}$, because the ion adsorption occurs inside the shear plane [30]. Zeta potential can be used to indirectly distinguish inner-sphere or outer-sphere surface adsorption for adsorbate adsorption on adsorbent [31]. Wang et al. [32] studied uranium adsorption by manganese oxides using zeta potential and pointed out uranium was adsorbed as cationic or neutral inner-sphere surface complexes. Inner-sphere adsorption for $Cu^{2+}$ adsorption

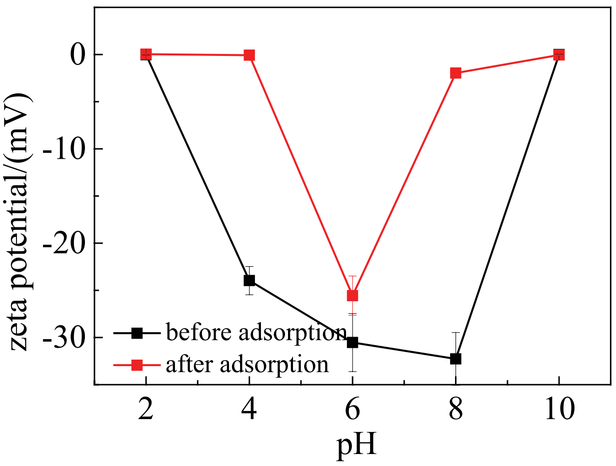

Fig. 4 The change of zeta potential before and after adsorption.

by activated sludge was found according to the change of zeta potential values toward positive direction by Jian et al. [29]. All of the zeta potential values after adsorption shifted positively at the pH range of 2–10 (Fig. 4). The increased zeta potential indicates E2 was adsorbed as cationic forms or neutral inner-sphere surface complexes which neutralized the negative electrostatic charges on adsorbent surface.

## 4. Conclusion

High adsorption intensity and binding force were exited between E2 and ZVI/AnGS, resulting in a high adsorption capacity of ZVI/AnGS to E2. The optimized condition was pH 6 with a high E2 adsorption efficiency of 92.78% and a high adsorption rate of 0.07 g·μg$^{-1}$·min$^{-1}$. E2 adsorption by ZVI/AnGS was an inner-sphere surface adsorption, and the adsorption rate was controlled by film diffusion or intraparticle diffusion. E2 adsorption process was suitably described by pseudo-second-order model. Freundlich and Langmuir isotherms were both suitable to describe the adsorption equilibrium process, which was exothermic and spontaneous. E2 was adsorbed as cationic forms or neutral inner-sphere surface complexes at the pH range of 2–10.

## Acknowledgments

The authors gratefully acknowledge Key Laboratory for Water Pollution Control and Wastewater Reuse in Anhui Province, the National Natural Science Foundation of China (51308010 and 51578002), and the Outstanding Youth Team Foundation of Ministry of Municipal Party committee in Beijing (Q0004018201502).

## References

[1] D. Belhaj, I. Jaabiri, H. Ayadi, M. Kallel, J.L. Zhou, Occurrence and removal of steroidal estrogens in Centre Eastern Tunisia municipal sewage treatment plant, Desal. Wat. Treat., 52 (2014) 2330–2339.

[2] M.J. Lust, R.M. Ziels, S.E. Strand, H.L. Gough, H.D. Stensel, Biodegradation kinetics of 17 alpha-ethinylestradiol in activated sludge treatment processes, Environ. Eng. Sci., 32 (2015) 637–646.

[3] Y.M. Li, Q.L. Zeng, S.J. Yang, Removal and fate of estrogens in an anaerobic-anoxic-oxic activated sludge system, Water Sci. Technol., 63 (2011) 51–56.

[4] L. Gonzalez-Gil, M. Papa, D. Feretti, E. Ceretti, G. Mazzoleni, N. Steimberg, R. Pedrazzani, G. Bertanza, J.M. Lema, M. Carballa, Is anaerobic digestion effective for the removal of organic micropollutants and biological activities from sewage sludge?, Water Res., 102 (2016) 211–220.

[5] X.H. Yu, J.C. Xue, H. Yao, Q. Wu, A.K. Venkatesan, R.U. Halden, K. Kannan, Occurrence and estrogenic potency of eight bisphenol analogs in sewage sludge from the US EPA targeted national sewage sludge survey, J. Hazard. Mater., 299 (2015) 733–739.

[6] X.J. Tang, Naveedullah, M.Z. Hashmi, H. Zhang, M.R. Qian, C.N. Yu, C.F. Shen, Z.H. Qin, R.L. Huang, J.N. Qiao, Y.X. Chen, A preliminary study on the occurrence and dissipation of estrogen in livestock wastewater, Bull. Environ. Contam. Toxicol., 90 (2013) 391–396.

[7] W. Zheng, X.L. Li, S.R. Yates, S.A. Bradford, Anaerobic transformation kinetics and mechanism of steroid estrogenic hormones in dairy lagoon water, Environ. Sci. Technol., 46 (2012) 5471–5478.

[8] V.M. Monsalvo, J.A. McDonald, S.J. Khan, P. Le-Clech, Removal of trace organics by anaerobic membrane bioreactors, Water Res., 49 (2014) 103–112.

[9] M. Carballa, F. Omil, J.M. Lema, M. Llompart, C. Garcia-Jares, I. Rodriguez, M. Gomez, T. Ternes, Behavior of pharmaceuticals, cosmetics and hormones in a sewage treatment plant, Water Res., 38 (2004) 2918–2926.

[10] A. Chiavola, P. Tedesco, M.R. Boni, Fate of some endocrine disruptors in batch experiments using activated and inactivated sludge, Water, Air, Soil Pollut., 227 (2016) 424.

[11] X.Y. Zheng, Y.J. He, W. Chen, M.Y. Wang, S.L. Cao, M. Ni, Y. Chen, A comparative adsorption study: 17 beta-estradiol onto aerobic granular sludge and activated sludge, Environ. Technol., 37 (2016) 136–144.

[12] Q.L. Zeng, Y.M. Li, G.W. Gu, Nitrate-dependent degradation of 17 alpha-ethinylestradiol by acclimated activated sludge under anaerobic conditions, J. Chem. Technol. Biotechnol., 84 (2009) 1841–1847.

[13] Y.X. Ren, K. Nakano, M. Nomura, N. Chiba, O. Nishimura, A thermodynamic analysis on adsorption of estrogens in activated sludge process, Water Res., 41 (2007) 2341–2348.

[14] X. Chen, J.Y. Hu, Adsorption of natural estrogens and their conjugates by activated sludge, Water, Air, Soil Pollut., 206 (2010) 251–261.

[15] B.H. Zhao, J.Y. Zhai, J. Chen, W. Bian, J. Li, Influence, equilibrium, thermodynamic and kinetic investigations on adsorption of 17beta-estradiol by anaerobic granule sludge, Desal. Wat. Treat., 79 (2017) 329–337.

[16] M. Clara, B. Strenn, E. Saracevic, N. Kreuzinger, Adsorption of bisphenol-A, 17 beta-estradiole and 17 alpha-ethinylestradiole to sewage sludge, Chemosphere, 56 (2004) 843–51.

[17] J.R. Cheng, X.M. Liu, Z.Y. Chen, Methane production from rice straw hydrolysate treated with dilute acid by anaerobic granular sludge, Appl. Biochem. Biotechnol., 178 (2016) 9–20.

[18] J. Zhang, G.P. Yang, Q. Li, X.Y. Cao, G.X. Liu, Study on the sorption behaviour of estrone on marine sediments, Mar. Pollut. Bull., 76 (2013) 220–226.

[19] T. Urase, T. Kikuta, Separate estimation of adsorption and degradation of pharmaceutical substances and estrogens in the activated sludge process, Water Res., 39 (2005) 1289–1300.

[20] Z.H. Zhang, Y.J. Feng, P. Gao, J.F. Liu, N.Q. Ren, Comparing the adsorption and desorption characteristics of 17 alpha-ethinylestradiol on sludge derived from different treatment units, Int. J. Environ. Sci. Technol., 9 (2012) 247–256.

[21] L. Zhu, J. Jin, H.Z. Lin, K.T. Gao, X.Y. Xu, Succession of microbial community and enhanced mechanism of a ZVI-based anaerobic granular sludge process treating chloronitrobenzenes wastewater, J. Hazard. Mater., 285 (2015) 157–166.

[22] B.H. Zhao, J.Y. Zhai, W. Bian, J. Zhang, Z.Z. Wang, Y. Li, J. Li, Enhanced adsorption behavior of 17β-estradiol by anaerobic granular sludge combined with zero-valent iron, J. Chem. Technol. Biotechnol., (2017), doi: 10.1002/jctb.5427.

[23] H.T. Dinh, J. Kuever, M. Mussmann, A.W. Hassel, M. Stratmann, F. Widdel, Iron corrosion by novel anaerobic microorganisms, Nature, 427 (2004) 829–832.

[24] W. Zhang, L. Chen, H. Chen, S.Q. Xia, The effect of $Fe^{-0}/Fe^{2+}/Fe^{3+}$ on nitrobenzene degradation in the anaerobic sludge, J. Hazard. Mater., 143 (2007) 57–64.

[25] C. Nguyen, D.D. Do, The Dubinin-Radushkevich equation and the underlying microscopic adsorption description, Carbon, 39 (2001) 1327–1336.

[26] H. Chen, G.L. Dai, J. Zhao, A.G. Zhong, J.Y. Wu, H. Yan, Removal of copper(II) ions by a biosorbent – *Cinnamomum camphora* leaves powder, J. Hazard. Mater., 177 (2010) 228–236.

[27] V. Padmavathy, Biosorption of nickel (II) ions by Baker's yeast: kinetic, thermodynamic and desorption studies, Bioresour. Technol., 99 (2008) 3100–3109.

[28] K.R. Krishna, L. Philip, Adsorption and desorption characteristics of lindane, carbofuran and methyl parathion on various Indian soils, J. Hazard. Mater., 160 (2008) 559–567.

[29] M. Jian, C. Tang, M. Liu, Dried biomass of activated sludge for $Cu^{2+}$ adsorption: behaviors and mechanisms, J. Dispersion Sci. Technol., 35 (2014) 1468–1475.

[30] W.G. Stumm, J.J. Morgan, Aquatic Chemistry: Chemical Equilibria and Rates in Natural Waters, 3rd ed., John Wiley & Sons, New York, 2012.

[31] M. Del Nero, C. Galindo, R. Barillon, E. Halter, B. Made, Surface reactivity of alpha-Al(2)O(3) and mechanisms of phosphate sorption: in situ ATR-FTIR spectroscopy and zeta potential studies, J. Colloid Interface Sci., 342 (2010) 437–444.

[32] Y.F. Guo, N.Q. Yan, P. Liu, S.J. Yang, J. Wang, Z. Qu, Removal of elemental mercury with Mn/Mo/Ru/$Al_2O_3$ membrane catalytic system, Front. Environ. Sci. Eng., 7 (2013) 464–473.